

Alternative reliability-based methodology for evaluation of structures excited by earthquakes

J. Ramon Gaxiola-Camacho^{*1}, Achintya Haldar^{2a}, Alfredo Reyes-Salazar^{1b}, Federico Valenzuela-Beltran^{3c}, G. Esteban Vazquez-Becerra^{4d} and A. Omar Vazquez-Hernandez^{5e}

¹Facultad de Ingeniería, Universidad Autónoma de Sinaloa, Culiacán, Sinaloa, México

²Department of Civil Engineering and Engineering Mechanics, University of Arizona, Tucson, Arizona, USA

³Instituto de Ingeniería, Universidad Nacional Autónoma de México, Coyoacán, Ciudad de México, México

⁴Facultad de Ciencias de la Tierra y el Espacio, Universidad Autónoma de Sinaloa, Culiacán, Sinaloa, México

⁵Department de Exploración de Aguas Profundas, Instituto Mexicano del Petróleo, G. A. Madero, Ciudad de México, México

(Received November 21, 2017, Revised March 10, 2018, Accepted March 11, 2018)

Abstract. In this paper, an alternative reliability-based methodology is developed and implemented on the safety evaluation of structures subjected to seismic loading. To effectively elaborate the approach, structures are represented by finite elements and seismic loading is applied in time domain. The accuracy of the proposed reliability-based methodology is verified using Monte Carlo Simulation. It is confirmed that the presented approach provides adequate accuracy in calculating structural reliability. The efficiency and robustness in problems related to performance-based seismic design are verified. A structure designed by experts satisfying all post-Northridge seismic design requirements is studied. Rigidities related to beam-to-column connections are incorporated. The structure is excited by three suites of ground motions representing three performance levels: immediate occupancy, life safety, and collapse prevention. Using this methodology, it is demonstrated that only hundreds of deterministic finite element analyses are required for extracting reliability information. Several advantages are documented with respect to Monte Carlo Simulation. To showcase an applicability extension of the proposed reliability-based methodology, structural risk is calculated using simulated ground motions generated via the broadband platform developed by the Southern California Earthquake Center. It is validated the accuracy of the broadband platform in terms of structural reliability. Based on the results documented in this paper, a very solid, sound, and precise reliability-based methodology is proved to be acceptable for safety evaluation of structures excited by seismic loading.

Keywords: reliability analysis; performance-based seismic design; limit state functions; Monte Carlo Simulation; artificial ground motions

1. Introduction

Currently, the safety evaluation of structures is becoming one of the most important concerns of structural engineers around the world. To avoid unexpected failures, the proper integrity of structures must be guaranteed when they are subjected to several loading conditions. Among many loadings affecting structural systems, demands produced by earthquakes represent a real challenge that professional engineers face daily during the design process;

particularly in seismic prone regions. In terms of economic losses, major earthquakes as 1989 Loma Prieta, 1994 Northridge, and 1995 Kobe produced damages of about 6, 30, and 200 billion USD, respectively. These costs questioned principally the fact that designing structures following prescriptive codes would guarantee their proper performance when excited by seismic loading. By the end of the nineties, as part of tremendous efforts done by scholars and professional engineers, the Federal Emergency Management Agency (FEMA) funded several projects to develop guidelines for stronger seismic design of structures, and to propose an alternative design criterion considering adverse economic consequences. The findings were published in a series of technical reports (FEMA-350 2000, FEMA-351 2000, FEMA-352 2000, FEMA-353 2000, FEMA-355C 2000, FEMA-355F 2000). One of the principal results was the introduction of an original design paradigm, generally known as Performance-Based Seismic Design (PBSD), representing an alternative to the life safety design concept employed in prescriptive code provisions. In the authors' opinion, to implement PBSD and any other seismic-resistant methodology, it is necessary to compute the corresponding reliability by applying the seismic loading in time domain in the presence of various sources of

*Corresponding author, Professor

E-mail: jrgaxiola@uas.edu.mx

^aProfessor

E-mail: haldar@email.arizona.edu

^bProfessor

E-mail: reyes@uas.edu.mx

^cPh.D. Candidate

E-mail: fvalenzuelab@iingen.unam.mx

^dProfessor

E-mail: gvazquez@uas.edu.mx

^eProfessor

E-mail: ovazquez@imp.mx

nonlinearity and uncertainty. Recently, several guidelines and recommendations have been published in the literature for the design of seismic resilient structures. In engineering practice, some of the most important are: *An Alternative Procedure for Seismic Analysis and Design of Tall Buildings Located in the Los Angeles Region* (LATBSDC 2011), *Guidelines for Performance-Based Seismic Design of Tall Buildings* (TBI 2010), *Seismic Provisions for Structural Steel Buildings* (AISC 341-10 2010), *Seismic Performance Assessment of Buildings* (FEMA P-58 2012), *NEHRP Recommended Seismic Provisions: Design Examples* (FEMA P-751 2012), and *Seismic Evaluation and Retrofit of Existing Buildings* (ASCE/SEI 41-13 2014). These recommendations and guidelines represent a considerable advancement in earthquake-resistant design. However, in certain aspects, the above guidelines cannot be used to satisfy the objectives of this paper. The main knowledge gap remains in estimating explicitly the structural reliability considering major sources of nonlinearities and uncertainties, applying seismic loading in time domain. Hence, an alternative methodology is necessary for structural safety evaluation. The authors support the idea that to introduce a reliability-based methodology for safety evaluation of structures excited by seismic loading, several important issues must be addressed as discussed next.

The performance level selection and appropriate mathematical models to represent structural behavior may be very complicated. When seismic loading is applied in time domain, it is expected that the structure develops multiple sources of nonlinearities, and the mathematical model to incorporate such nonlinear behavior could be considerably demanding. To study nonlinear behavior, it is common to represent structures using Finite Elements (FEs). To capture the dynamic application of the seismic loading, several methods with various degrees of difficulty are recommended in up-to-date design guidelines, including pseudo-static to time domain application of the excitation (ASCE/SEI 7-16 2017). The most precise nonlinear analysis will require a structure to be represented by nonlinear FEs applying seismic loading in time domain. The proper application of seismic loading in time domain depends on the selection of ground motions, such ground motions must represent the seismic hazard of the zone where the structure will be located. Commonly used construction codes recommend the use of eleven or more ground motions to perform time domain analysis (ASCE/SEI 7-16 2017). In addition, it is reported that time domain analysis can be performed using real (recorded) or artificial (simulated) ground motions, depending on the availability of records in the zone. Once representative ground motions are selected, time history analysis can be performed following the recommendations reported in building codes (ASCE/SEI 7-16 2017). However, the main challenge in the profession remains in the explicit quantification of the vulnerability (reliability) of structures to future seismic loading. Besides, commonly used analytical models of nonlinear structures are too idealized and may not satisfy the underlying physics. For example, joints and support conditions in structures are rarely Fully Restrained (FR); they are

essentially Partially Restrained (PR) with different rigidities (Chen and Kishi 1989, Colson 1991, Elsati and Richard 1996, Reyes-Salazar and Haldar 1999, Reyes-Salazar *et al.* 2016a). Beam-to-column connections introduce nonlinearity in the structural response, and structural dynamic properties (damping, mode shape, frequency, stiffness, etc.) are expected to be quite different if the connection conditions are modeled realistically. The main point is that the above desirable performance-enhancing features must be incorporated in developing an alternative reliability-based methodology for safety evaluation of structures excited by seismic loading. In terms of reliability theory, structural risk can be calculated using the First Order Reliability Method (FORM) (Haldar and Mahadevan 2000a). This methodology can be implemented only if the required Limit State Function (LSF) is available in explicit form, and its derivatives with respect to the design variables can be calculated. Unfortunately, for nonlinear structures excited by seismic loading in time domain, LSFs are expected to be implicit, and the implementation of FORM can be very complicated. As an option, Monte Carlo Simulation (MCS) may be utilized for the structural risk calculation. However, it is demonstrated that MCS may not be efficient for seismic analysis of structures in time domain. Although many sophisticated space reduction techniques can be implemented in MCS, it requires an excessive amount of computational time (Haldar and Mahadevan 2000b).

Considering the above issues, five objectives motivate and justify the research presented in this paper: (1) To develop an alternative reliability-based methodology for implicit LSFs considering major sources of nonlinearity and uncertainty applying seismic loading in time domain, (2) to evaluate the appropriateness of the proposed reliability-based methodology to be implemented in PBSD of structures, (3) to incorporate performance enhancing features like rigidities of beam-to-column connections in the proposed reliability evaluation method, (4) to demonstrate the applicability of the reliability-based methodology using site-specific simulated ground motions in time domain, and (5) to showcase the implementation potential of the reliability-based methodology with the help of numerical examples.

2. Concept of reliability analysis

The concept of reliability analysis is maturing and several techniques have been reported in the literature to estimate risk (Haldar and Mahadevan, 2000a, b). In general terms, the underlying structural safety is computed by a deterministic approach based on a safety factor concept. However, since the intended conservatism introduced depends on the uncertainty in the load and resistance of the structure, and the experience of structural engineers, safety factor approaches may fail to convey the actual margin of safety in structures. Consequently, more rational approaches must be used to explicitly compute the margin of safety considering uncertainties related to load and resistance variables. Since uncertainties in load and resistance variables should be considered in reliability analysis, it may

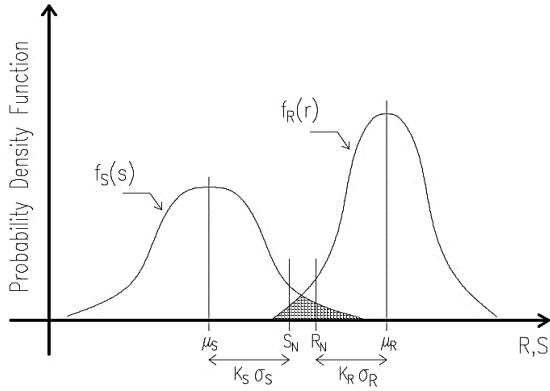


Fig. 1 Illustration of reliability analysis concept

be difficult to satisfy the basic design requirements during the evaluation. A simple case of reliability analysis is illustrated in Fig. 1. It can be observed in Fig. 1 that two variables are considered, one related to the demand on the system (e.g., loads acting in a structure, S) and the other related to the capacity of the system (e.g., resistance of the structure, R). Both S and R are random in nature. They are randomly characterized by mean values (μ_S and μ_R), standard deviations (σ_S and σ_R), and corresponding probability density functions [$f_S(s)$ and $f_R(r)$]. The nominal (deterministic) values of load and resistance are illustrated in Fig. 1 as S_N and R_N , respectively. Nominal values are used in conventional safety factor approach and depend on the parameters K_S and K_R defining the level of conservatism in the design.

Generally, the intent of conventional approaches can be explained by considering the overlapped or shaded area between both curves $f_S(s)$ and $f_R(r)$ as shown in Fig. 1. The shaded region in Fig. 1 represents the probability of failure (p_f), which depends on three factors of the two curves: (1) relative position between them depending on the mean values (μ_S and μ_R), (2) dispersion among curves given by the standard deviations (σ_S and σ_R), and (3) shapes of the two curves represented by the corresponding Probability Density Function (PDF). Hence, deterministic design procedures achieve safety by selecting design variables in such way that the shaded area between $f_S(s)$ and $f_R(r)$ is as small as possible. As stated earlier, deterministic approaches generally shift the position of $f_S(s)$ and $f_R(r)$ using safety factors. However, a more rational approach would be to calculate the underlying risk by considering the above three factors (μ , σ and PDF). Thus, design variables would be selected satisfying an acceptable risk. To clarify this concept, the failure state of structural systems can be represented as

$$g(R, S) = R - S < 0 \quad (1)$$

where $g(R, S)$ is the mathematical representation of the relationship of Random Variables (RVs).

The failure event $P(R < S)$ or p_f represents the shaded area (Ω) in Fig. 1. It can be calculated by computing the overlapped area (Ω) between $f_S(s)$ and $f_R(r)$ as

$$p_f = P(R < S) = P[g(R, S) < 0]$$

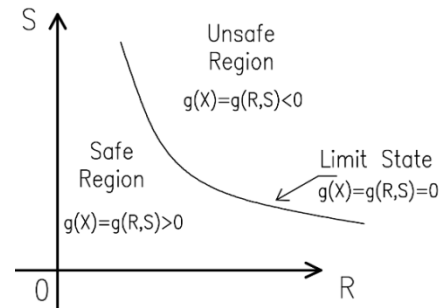


Fig. 2 Limit state concept

$$= \iint_{\Omega} f_{R,S}(r, s) dr ds \quad (2)$$

where $f_{R,S}(r, s)$ is the joint PDF of the RVs related to resistance and load.

The integration of Eq. (2) is performed over the failure region (Ω). Generally, RVs related to S and R are function of several variables as gravity, lateral, and accidental loads, and/or sectional and material properties. Hence, Eq. (1) can be expressed in terms of multiple RVs as

$$g(\mathbf{X}) = g(x_1, x_2, \dots, x_k) \quad (3)$$

where \mathbf{X} is a vector that represents the load and resistance RVs (x_1, x_2, \dots, x_k), and k is the number of RVs.

Based on the above discussion, the LSF can be defined as $g(\mathbf{X}) = 0$. This represents the boundary between the safe and unsafe region in the design parameter space, i.e., the state of a structure representing the limit between the appropriate and inappropriate performance. The LSF and the safe and unsafe regions are illustrated in Fig. 2 in terms of R and S . The LSF plays an important role in the calculation of reliability or risk. As previously mentioned, LSFs can be explicit or implicit functions in terms of RVs. Combining Eqs. (2) and (3), and considering that failure occurs when $g(\mathbf{X}) < 0$, the p_f can be calculated as

$$p_f = \int \dots \int_{g(\mathbf{X}) < 0} f_{\mathbf{X}}(x_1, x_2, \dots, x_k) dx_1 dx_2 \dots dx_k \quad (4)$$

where $f_{\mathbf{X}}(x_1, x_2, \dots, x_k)$ is the joint PDF related to the basic RVs represented by the vector \mathbf{X} .

The integration represented by Eq. (4) is performed over the failure region [$g(\mathbf{X}) < 0$]. If the RVs are statistically independent, the joint PDF can be replaced in Eq. (4) by the product of individual PDFs. However, PDFs of RVs are difficult to obtain, and even if they were available, solving multiple integrals as presented in Eq. (4) can be extremely complicated. Hence, an alternative is to use analytical approximations to solve the integral represented by Eq. (4). Unfortunately, analytical approximations are often restricted to use only the mean (μ) and coefficient of variation (COV) because the information about RVs may only be sufficient to evaluate μ and COV (Ang and Cornell 1974). This prompted to the development of the Mean Value First-Order Second-Moment (MVFOSM) method. However, MVFOSM fails to consider the distributional information of RVs. This issue was addressed in the literature by introducing FORM

(Haldar and Mahadevan 2000a, b). Hence, FORM will be integrated in the alternative reliability-based methodology proposed in this paper for safety evaluation of structures excited by seismic loading.

3. Requirements in reliability methods for structures excited by seismic loading

Generally, the engineering profession uses FE formulations to study the seismic behavior of structures as realistically as possible. The most rigorous FE analysis requires the proper application of seismic loadings in time domain. The phrase “probability of failure” or “probability of not satisfying a performance requirement” implies that the risk needs to be evaluated just before failure in the presence of several sources of nonlinearities. In general, three conditions must be considered for the proper calculation of p_f : (1) structures must be represented by FEs, (2) seismic loading must be applied in time domain, and (3) major sources of nonlinearity and uncertainty must be considered related to material properties, large deformations and rigidity of connections. The seismic performance of structures can be represented by LSFs, which are expressed in terms of RVs. The LSFs depend on prescribed performance requirements. As previously discussed, if LSFs are explicitly available, FORM can be used directly for seismic risk evaluations. However, for nonlinear structures subjected to seismic loading applied in time domain, LSFs are expected to be implicit and function of time. As stated earlier, for implicit LSFs, one of the reliability evaluation methods that can be used is MCS. However, for structures excited by ground motion time histories, one deterministic analysis can take about 4 minutes. In addition, to calculate p_f of about the order of 10^{-5} , around 1 million simulations will be necessary (Haldar and Mahadevan 2000a, b). For example, if 10,000 MCS are used, it will require 40,000 minutes, or about 28 days of continuously running of a computer. Thus, the basic MCS is not practical. To overcome the above issues, an alternative reliability-based methodology will be proposed, validated, and applied to the evaluation of earthquake-resistant structures, using both real and simulated ground motions.

4. Simulation of ground motions

It was documented earlier that commonly used building codes (ASCE/SEI 7-16 2017) recommend the use of at least eleven ground motions for structural seismic analysis. Such ground motions can be simulated (artificial) and/or recorded (real). However, the main question raised by the profession related to the above issue is: what would be the associated risk of structures when they are subjected to artificial in comparison with real ground motions? This represents another knowledge gap in implementing adequate safety evaluation methods. To solve this concern, the engineering profession needs to have two approaches: (1) a technique for the proper generation of artificial ground motions, and (2) a reliability-based framework to compute the seismic risk of structures. As will be documented in the next section

of this paper, the proposed alternative reliability-based methodology will represent a good option for the calculation of seismic risk of structures. On the other hand, several techniques have been proposed in the literature for the simulation of ground motions (Shinozuka and Deodatis 1988, Suarez and Montejo 2005, Cacciola and Deodatis 2011, Cacciola and Zentner 2012, Yamamoto and Baker 2013, Shields 2014, Burks *et al.* 2015, SCEC 2016). Among them, the Broadband Platform (BBP) developed by the Southern California Earthquake Center (SCEC) (SCEC, 2016) will be used in this study for the simulation of ground motions, and its implementation in safety evaluation will be documented in terms of structural risk.

5. Alternative reliability-based methodology

In general terms, the proposed alternative reliability-based methodology works iteratively to calculate the reliability index (β), Most Probable Failure Point (MPFP) and p_f . The reliability framework is explained in this section in terms of seven items: (1) advanced experimental design, (2) finite element evaluation, (3) polynomial representation, (4) limit state functions, (5) first order reliability method, (6) uncertainties in structures excited by seismic loading, and (7) structural safety evaluation.

5.1 Advanced experimental design

The first step in the iterative framework of the alternative reliability-based methodology is to define the experimental design. During every iteration, an experimental design should be defined depending on the desired accuracy and efficiency. To properly generate the LSF under consideration, an advanced experimental design is proposed integrating Saturated Design (SD) and Central Composite Design (CCD) (Khuri and Cornell 1996). SD is less accurate, but it provides more efficiency since it requires the same amount of deterministic FE analyses (sampling points) as the total number of unknown coefficients necessary to define the LSF in terms of a polynomial (polynomials are discussed later in this paper). Such unknown coefficients are obtained by solving a set of linear equations. In addition, a second-order polynomial without and with cross terms can be used to generate the LSF requiring $2k + 1$ and $(k + 1)(k + 2)/2$ number of deterministic FE analyses, respectively; where k was defined earlier as the number of RVs. Conversely, CCD is more accurate but less efficient since it generates the LSF in terms of a second-order polynomial with cross terms and regression analysis is required to calculate the unknown coefficients. One center point, two axial points located on the axis of each RV at a distance equal to $\sqrt[4]{2^k}$ measured from the center point, and 2^k factorial points are necessary to define CCD. Hence, the total number of deterministic FE analyses in CCD is equal to $2^k + 2k + 1$. More information about SD and CCD is widely reported in the literature (Box *et al.* 1978, Faravelli 1989, Khuri and Cornell 1996) and is beyond the scope of this paper. Since the alternative reliability-based methodology is iterative, during the first and intermediate iterations, sampling points will be selected

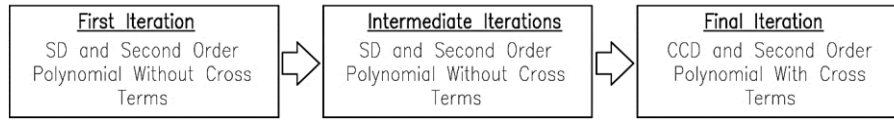


Fig. 3 Experimental designs of the alternative reliability-based methodology.

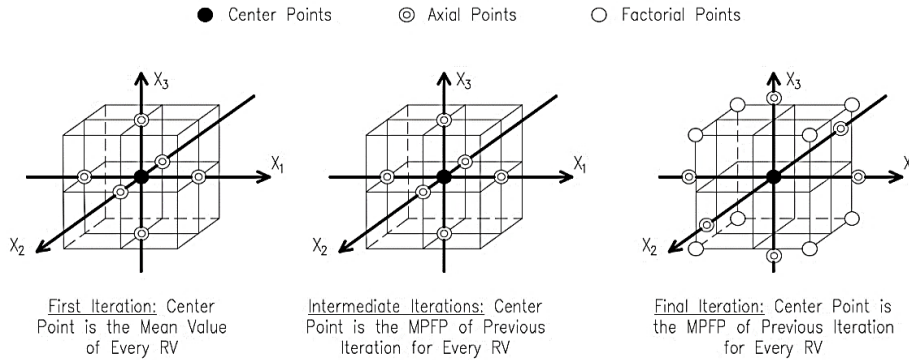


Fig. 4 Center point selection for every iteration considering three RVs (X_1, X_2 and X_3).

using SD, and the LSF will be generated in terms of a second order polynomial without cross terms. This will provide the required efficiency. For the last iteration, accuracy will be incorporated using CCD to generate the final LSF using a second order polynomial with cross terms. Fig. 3 illustrates the process in terms of experimental designs.

To define the sampling region, during every iteration, depending on the experimental design used, sampling points (X_{ij}) will be selected around a center point (X_i^C) as

$$X_{ij} = X_i^C \pm h_i x_{ij} \sigma_{X_i} \quad (5)$$

$i = 1, 2, \dots, k \quad \text{and} \quad j = 1, 2, \dots, N$

where k is the number of RVs; N is the number of experimental sampling points; σ_{X_i} is the standard deviation of a RV X_i ; h_i is an arbitrary factor that defines the experimental region; and x_{ij} is the coded variable.

The selection of the center point (X_i^C) is very important. For the first iteration, the center point (X_i^C) will be considered as the mean value (μ_{X_i}) of the corresponding RV. For intermediate and final iterations, the center point (X_i^C) will be considered as the coordinates of the MPFP (x_i^*) of the previous iteration. To clarify the process of selection of sampling points, Fig. 4 is introduced. Center point selection in terms of three RVs (X_1, X_2 and X_3) is illustrated in Fig. 4.

5.2 Finite element evaluation

Once experimental points are selected, they will be used for finite element evaluations. This represents an essential part of the alternative reliability-based methodology. Considering its numerous advantages, the stress-based Finite Element Method (FEM) is used for the calculation of deterministic seismic responses (Reyes-Salazar and Haldar 1999). A comprehensive explanation of the theoretical foundation of the FEM algorithm is beyond the scope of this paper. Thus, only the necessary features that directly pertain to this research are briefly discussed in this section.

The complete formulation of the assumed stress-based FEM can be found in the literature (Reyes-Salazar and Haldar 1999, Mehrabian *et al.* 2005, Mehrabian *et al.* 2009, Reyes-Salazar *et al.* 2014, Reyes-Salazar *et al.* 2016b, Gaxiola-Camacho *et al.* 2017, Azizoltani and Haldar 2017a, b, Azizoltani *et al.* 2018). Basically, the assumed stress-based FEM is used in this paper to calculate deterministic nonlinear responses of structures in the presence of FR and PR beam-to-column connections, applying seismic loading in time domain. The sources of nonlinearity considered in the algorithm are due to large deformations, material properties, and beam-to-column connections. For nonlinear deformations, second order effects are considered related to the structure and members distortions, respectively. Material nonlinearity is incorporated in the formulation as a result of the constitutive relationship of the material, it will be considered to be elastic-perfectly plastic (Hinton and Owen, 1986). Nonlinearity produced by rigidities related to PR beam-to-column connections is incorporated in the algorithm using the 4-parameters Richard Model (Mehrabian *et al.* 2005, Mehrabian *et al.* 2009). This model represents the moment-rotation ($M-\theta$) curve of beam-to-column connections using four parameters related to the connection type: initial stiffness (K), plastic stiffness (K_p), reference moment (M_0), and curve shape parameter (N_C) (Elsati and Richard 1996). In terms of safety evaluation of structures subjected to seismic loading, one of the main contributions of this paper is that all the above enhancing features are incorporated in the alternative reliability-based methodology. This will be demonstrated later with the help of numerical examples.

After every single deterministic nonlinear finite element analysis is completed, a tremendous amount of data will be available in terms of nonlinear structural responses. In summary, the finite element evaluation works in the iterative process as illustrated in Fig. 5. Using the generated data, a polynomial will be constructed depending on the experimental design, corresponding iteration, and the LSF under consideration.

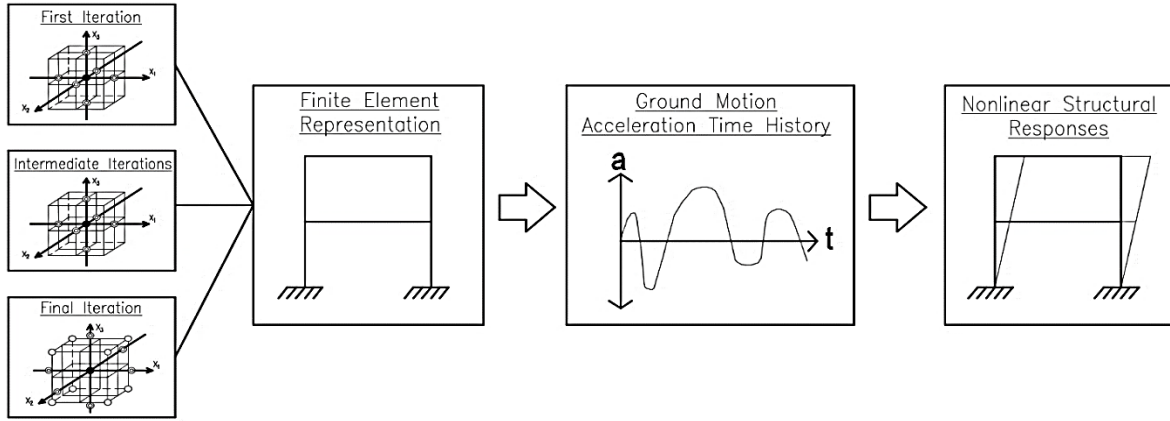


Fig. 5 Finite element evaluation

5.3 Polynomial representation

The polynomial representation of the LSF is fundamental in the proposed algorithm. In the context of seismic loading applied in time domain, it will be nonlinear. It is documented in the literature that the selection of more than second-order polynomials to represent a LSF can be very complicated (Khuri and Cornell 1996). In addition, the calculation effort increases together with the number of RVs involved in the risk evaluation. Considering several characteristics of polynomials and the dynamic responses of structures, the LSF under study will be represented by a second-order polynomial without or with cross terms as

$$\hat{g}(\mathbf{X}) = b_0 + \sum_{i=1}^k b_i X_i + \sum_{i=1}^k b_{ii} X_i^2 \quad (6)$$

and

$$\hat{g}(\mathbf{X}) = b_0 + \sum_{i=1}^k b_i X_i + \sum_{i=1}^k b_{ii} X_i^2 + \sum_{i=1}^{k-1} \sum_{j>1}^k b_{ij} X_i X_j \quad (7)$$

where X_i ($i=1,2,\dots,k$) is the i^{th} RV; k is the total number of RVs involved in the problem; b_0 , b_i , b_{ii} and b_{ij} are the unknown coefficients to be determined; and $\hat{g}(\mathbf{X})$ is the approximate LSF of the original $g(\mathbf{X})$.

5.4 Limit state functions

Considering that structures may fail due to excessive lateral deflection because of a major seismic excitation, overall lateral and inter-story drift LSFs need to be considered.

5.4.1 Overall lateral and inter-story drift

In general terms, LSFs represent functional relationships of load and resistance-related design variables. Theoretically, a LSF can be expressed as

$$g(\mathbf{X}) = \delta_{allow} - y_{max}(\mathbf{X}) = \delta_{allow} - \hat{g}(\mathbf{X}) \quad (8)$$

where δ_{allow} is the permissible or allowable displacement value corresponding to a specific performance requirement, $\hat{g}(\mathbf{X})$ is the polynomial representation of the behavior of the load and resistance-related design variables, and \mathbf{X} is a

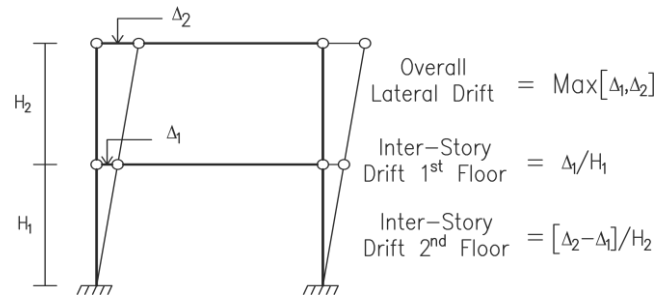


Fig. 6 Overall lateral and inter-story drift evaluation

vector in terms of the design variables. Two LSFs related to overall lateral and inter-story drifts (see Fig. 6) are reported as fundamental in the engineering profession (FEMA-350 2000, FEMA-351 2000, FEMA-352 2000, FEMA-353 2000, FEMA-355C 2000, FEMA-355F 2000). They will be studied later in the numerical validation of the proposed reliability-based methodology.

5.5 First order reliability method

The FORM evaluation incorporates distributional information of every single RV in the algorithm and helps to generate the polynomial in the failure region. FORM works iteratively following the next 8 steps.

- Step 1: Define the proper LSF in terms of a polynomial representation.
- Step 2: Assume the initial values of the design point (x_i^*). Generally, the initial values are taken as the mean values (μ_{x_i}) of every RV.
- Step 3: If there are non-normal distributed RVs, their equivalent normal standard deviation ($\sigma_{x_i}^N$) and mean ($\mu_{x_i}^N$) must be computed as

$$\sigma_{x_i}^N = \frac{\phi\{\Phi^{-1}[F_{x_i}(x_i^*)]\}}{f_{x_i}(x_i^*)} \quad (9)$$

and

$$\mu_{x_i}^N = x_i^* - \Phi^{-1}[F_{x_i}(x_i^*)] \sigma_{x_i}^N \quad (10)$$

where F_{x_i} and f_{x_i} are the non-normal distribution and density functions of X_i , respectively; Φ and ϕ are the Cumulative Density Function (CDF) and PDF of standard

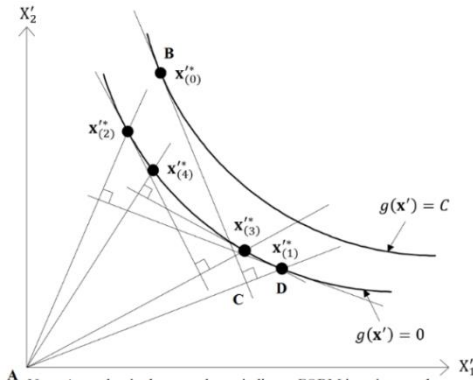


Fig. 7 FORM iteration process

RVs, respectively.

- Step 4: Evaluate $\left(\frac{\partial g}{\partial X_i}\right)^*$ and α_i for every x_i^* as

$$\alpha_i = \frac{\left(\frac{\partial g}{\partial X_i}\right)^*}{\sqrt{\sum_{i=1}^k \left(\frac{\partial g}{\partial X_i}\right)^{2*}}} \quad (11)$$

- Step 5: Obtain the new design point x_i^* in terms of β as

$$x_i^* = \mu_{X_i}^N - \alpha_i \beta \sigma_{X_i}^N \quad (i = 1, 2, \dots, k) \quad (12)$$

- Step 6: Substitute the new x_i^* in the LSF as $g(x^*) = 0$ and solve again for β .

- Step 7: Using the β value obtained in Step 6, reevaluate x_i^* .

- Step 8: Repeat Step 4 to 7 until β converges to a tolerance criterion (see Fig. 7)

Generally, FORM process calculates the *MPFP* and β as shown above (see Fig. 7). The FORM evaluation can be very time consuming if a great number of RVs is involved in the process. To increase efficiency, the number of RVs can be reduced considering only the most significant of them.

5.5.1 Reduction of RVs

Generally, the number of RVs considered during the risk evaluation determines the efficiency of the process. It is obvious that when the number of RVs (k) is large, CCD cannot be implemented. A measure called the sensitivity index can be used to quantify the influence of each RV (Haldar and Mahadevan 2000a, b). In the context of FORM, the sensitivity index of a variable X_i is the directional cosine $\alpha_i(X_i)$ of the unit normal variable at the checking or design point. This will be available from the FORM evaluation. RVs with low sensitivity index at the end of the first iteration can be treated as deterministic using their mean values in the subsequent iterations. The reduction of the total number of RVs significantly improves efficiency without compromising accuracy. The reduced number of RVs will be denoted hereafter as k_r . To clarify the importance of reduction of RVs, suppose that during the last iteration, CCD and $k = 30$ are used. Then, the required number of experimental sampling points or deterministic

FE evaluations, only for the last iteration, will be $2^k + 2 * k + 1 = 2^{30} + 2 * 30 + 1 = 1,073,741,885$. On the other hand, if a reduction in the number of RVs is performed and $k_r=7$ is used, the required number of experimental sampling points will be $2^{k_r} + 2 * k_r + 1 = 2^7 + 2 * 7 + 1 = 143$. It can be observed that if a reduction of RVs is performed, the number of deterministic FE evaluations can be substantially reduced. For clarification purposes, suppose that it will take three iterations to calculate the seismic risk of a structure. Then, if $k=30$ and $k_r=7$, the required number of experimental sampling points or deterministic FE evaluations will be $(2 * k + 1) + (2 * k_r + 1) + (2^{k_r} + 2 * k_r + 1) = (2 * 30 + 1) + (2 * 7 + 1) + (2^7 + 2 * 7 + 1) = 219$. Hence, the risk evaluation will require only hundreds instead of thousands or millions of deterministic FE evaluations.

5.6 Uncertainties in structures excited by seismic loading

Uncertainties related to both the structure and earthquake excitation should be considered in the seismic risk evaluation of structures. The alternative reliability-based methodology proposed in this paper incorporates uncertainties as discussed in this section. The uncertainties associated with resistance-related parameters are widely reported in the literature (Ellingwood 1980, Haldar and Mahadevan 2000a, b, Nowak and Collins 2012). The appropriate information is used in this paper. Later in this study, the alternative reliability-based methodology will be demonstrated by considering the seismic performance of several steel structures. All structural elements will be W-type sections reported in the Steel Construction Manual (AISC 2011). Young's modulus (E), yield stress of columns (F_y) and girders (F_y), cross sectional area (A), and moment of inertia (I_x) of W-type sections used for structural elements will be considered as RVs with a Lognormal distribution with *COV* of 0.06, 0.10, 0.10, 0.05, and 0.05, respectively. Gravity loads are classified as Dead Load (DL) and Live Load (LL). The uncertainties associated with both are available in the literature (Ellingwood 1980, Haldar and Mahadevan 2000a, b, Nowak and Collins 2012); similar information is used in this study. DL and LL are represented by a Normal and Type 1 distributions with *COV* of 0.10 and 0.25, respectively. As discussed before, the 4-Parameter Richard Model is used for the proper incorporation of connection rigidities in the algorithm. It has been reported in the literature (Haldar and Mahadevan 2000a, b) that the four parameters defining the 4-Parameter Richard Model are randomly distributed. The four parameters K , K_p , M_0 , and N_c will be considered as RVs with a Normal distribution and *COV* of 0.15, 0.15, 0.15, and 0.05, respectively. As previously documented, seismic loading needs to be applied in time domain. Consideration of uncertainties in seismic loading is very challenging and still evolving. Uncertainty associated with the intensity and the frequency contents needs to be considered. To incorporate the uncertainty in the intensity, a factor (g_e) is used in this study. It is considered as a RV with a Type 1 distribution and *COV* equal to 0.20. To incorporate uncertainty in the frequency contents, recent design

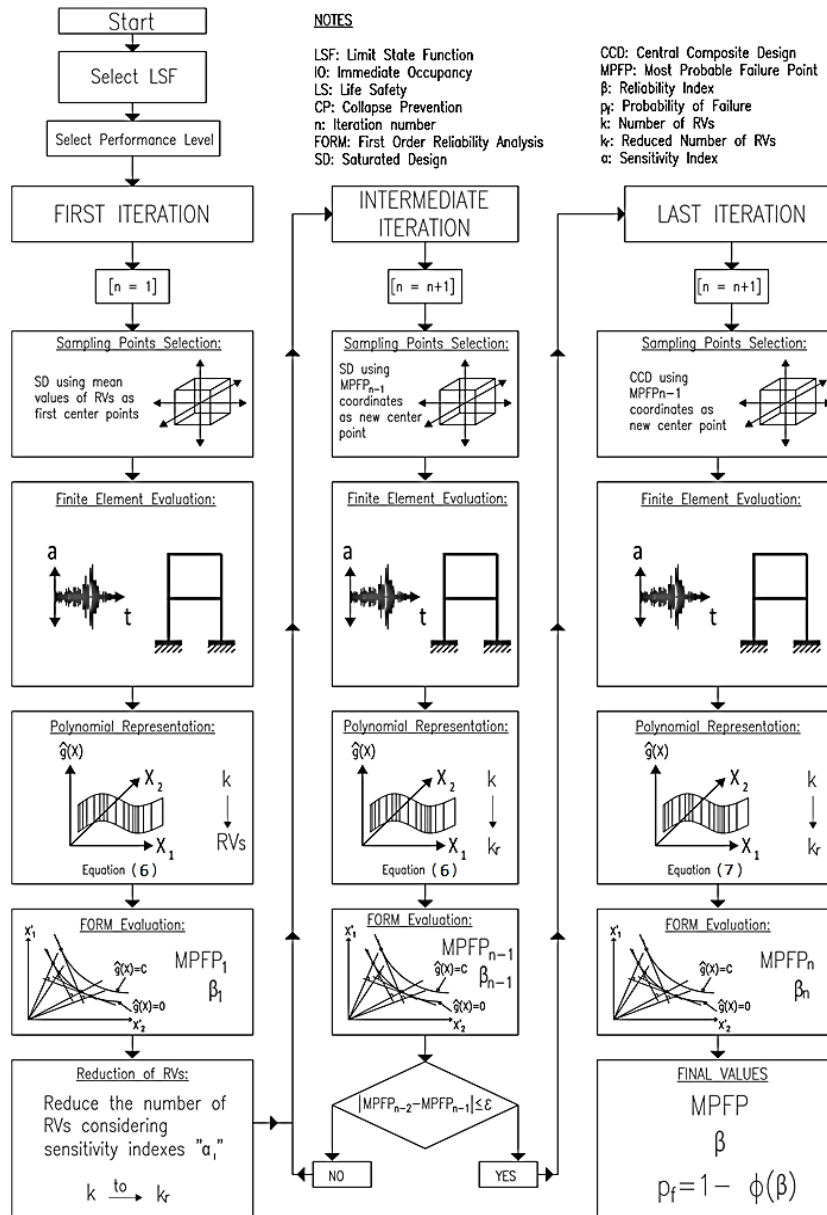


Fig. 8 Alternative reliability-based methodology flowchart

guidelines (ASCE/SEI 7-16 2017) suggest to considerate suites of at least eleven time histories expected for the location. In this paper, several ground motions with different frequency contents will be used for the reliability evaluation of structures.

5.7 Structural safety evaluation

In summary, the alternative reliability-based methodology appears to be challenging. In the proposed algorithm, the necessary response information will be generated calculating maximum seismic responses of structures using stress-based FEM and specific sampling points. In the first iteration, an approximation of the LSF will be generated using SD and Eq. (6). The mean values of all RVs in the normal variable space will be considered as center points. At the end of the first iteration, in the context of FORM, the first β , $MPFP$, and sensitivity indexes (α_i) of

all RVs will be available. Then, RVs with low sensitivity indexes will be considered as deterministic at their mean values and k will be reduced to k_r . The next iteration will start by using k_r number of RVs and the previously obtained $MPFP$ as center point. An updated LSF will be generated using SD and Eq. (6). Using the updated LSF, FORM will calculate β and $MPFP$. Then, the updated $MPFP$ will be used as center point for the next iteration. The overall updating in center points in terms of $MPFP$ will continue until β values for two consecutive iterations converge to a pre-established tolerance level. In the final iteration, CCD and Eq. (7) will be used to generate the final LSF, and its corresponding unknown coefficients will be obtained using regression analysis. In general, it usually takes three to four iterations to reach convergence in terms of β values. Once the final β value is found, the coordinates of the last checking point (x^*) or final $MPFP$ will be estimated as

$$\beta = \sqrt{(x^*)^t(x^*)} \quad (13)$$

Finally, based on the converged value of β , the corresponding p_f can be estimated as

$$p_f = \Phi(-\beta) = 1.0 - \Phi(\beta) \quad (14)$$

A flowchart of the alternative reliability-based methodology is illustrated in Fig. 8.

6. Numerical examples-Validation and application

To implement a new methodology, it is necessary to validate its capabilities in terms of accuracy and efficiency. In this section, verification is demonstrated by studying a 2-story steel frame, it is excited using two acceleration time histories recorded during the 1994 Northridge earthquake. Structural reliability is calculated using the alternative reliability-based methodology and the well-established MCS. To validate its implementation potential in PBSD, a 3-story steel structure is considered. Its associated seismic risk is calculated considering FR and PR connections, and several ground motions in terms of Immediate Occupancy (IO), Life Safety (LS), and Collapse Prevention (CP) performance levels. In addition, the structural risk of the 2-story steel frame is compared in terms of simulated and real ground motions.

6.1 Validation using monte carlo simulation

To validate the accuracy of the Alternative Reliability-Based Methodology (ARBM), a 2-story steel frame illustrated in Fig. 9(a) is considered. A reasonably small structure is studied to expedite the comparison of reliability estimations using the ARBM and standard MCS. As previously discussed, beam-to-column connections are considered to be either FR or PR type. Post-Northridge PR connections are considered for the risk evaluation as illustrated in Fig. 9(b).

These connections are characterized by two slots in the web of the beam; more information about these connections can be found in the literature (Mehrabian *et al.* 2005). The four parameters of the Richard model to analytically define post-Northridge connections are presented Table 1. The steel frame is excited using two time histories during 20 seconds as shown in Figs. 9(c)-(d). All RVs that are necessary to analyze the frame are summarized in Table 2. The information on uncertainty associated with them is also presented in Table 2. In Table 2, uncertainty is expressed in terms of mean value (\bar{X}), nominal value (X_N), mean to

nominal ratio (\bar{X}/X_N), COV, and distribution. For this numerical example, $k = 14$ and $k_r = 5$.

The reliability index, β , and p_f are estimated using the ARBM and MCS for both LSFs corresponding to overall

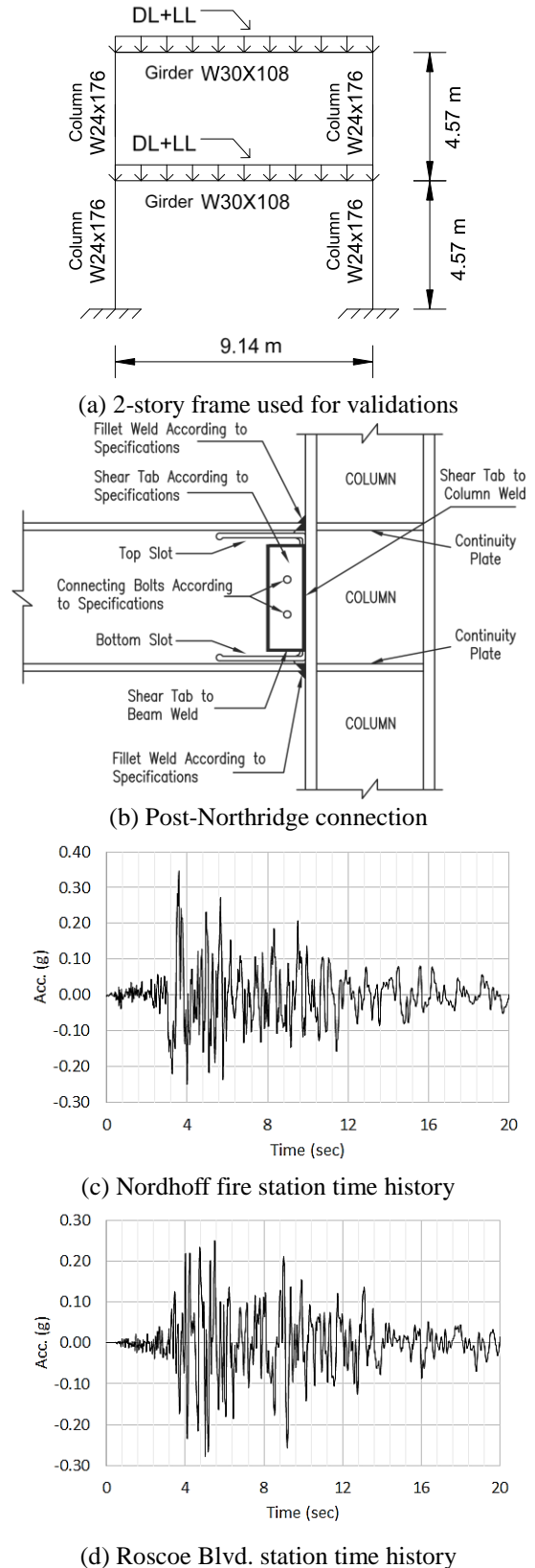


Fig. 9 Numerical example used for validation

Table 1 Post-Northridge 4-Richard parameters corresponding to 2-Story steel frame

4-Richard Parameters	PR post-Northridge Connection
K (kN-m/rad)	1.9546E+07
K_p (kN-m/rad)	4.5194E+03
M_0 (kN-m)	2.0145E+03
N_C	1.00

Table 2 Uncertainty of RVs used for 2-story steel frame

RV	Mean (\bar{X})	Nominal (X_N)	\bar{X}/X_N	COV	Distribution
E (kN/m ²)	1.9995E+08	1.9995E+08	1.00	0.06	Lognormal
F_y (kN/m ²)	3.6197E+05	3.4474E+05	1.05	0.10	Lognormal
A (m ²)	**	*	1.00	0.05	Lognormal
I_x (m ²)	**	*	1.00	0.05	Lognormal
DL (kN/m ²)	4.0219	3.8304	1.05	0.10	Normal
LL (kN/m ²)	1.1970	2.3940	0.50	0.25	Type 1
K (kN-m/rad)	***	*	1.00	0.15	Normal
K_p (kN-m/rad)	***	*	1.00	0.15	Normal
Mo (kN-m)	***	*	1.00	0.15	Normal
N_C	***	*	1.00	0.05	Normal
g_e	1.00	1.00	1.00	0.20	Type 1

*Nominal value (X_N) is calculated using mean value (\bar{X}) and \bar{X}/X_N .

**Mean values of A and I_x can be found in steel construction manual (AISC, 2011). They are considered RVs for every girder and column.

***Mean values of four Richard parameters are reported in Table 1.

Table 3 Reliability results for 2-Story steel frame

Ground Motion	LSF	Method	FR		PR (post-Northridge)	
			β (TNDA)	p_f	β (TNDA)	p_f
Nordhoff Fire Station	Overall Lateral	ARBM	3.6949 (94)	0.000110	3.8853 (94)	0.000051
		MCS	3.7190 (50,000)	0.000100	3.8461 (50,000)	0.000060
	Inter-story Drift	ARBM	3.2954 (94)	0.000491	3.5170 (94)	0.000218
		MCS	3.3139 (50,000)	0.000460	3.5149 (50,000)	0.000220
Roscoe Blvd Station	Overall Lateral	ARBM	3.6508 (94)	0.000131	3.9039 (94)	0.000040
		MCS	3.6331 (50,000)	0.000140	4.1075 (50,000)	0.000020
	Inter-story Drift	ARBM	3.2528 (94)	0.000571	3.5969 (94)	0.000161
		MCS	3.2585 (50,000)	0.000560	3.5985 (50,000)	0.000160

lateral and inter-story drift at the second-floor level, respectively. Beam-to-column connections are assumed to be FR and PR post-Northridge types. The permissible overall lateral and inter-story drift are 2.86 and 1.43 cm, respectively. The results in terms of β and p_f values for the two LSFs are summarized in Table 3. In Table 3, β and p_f are estimated using 50,000 cycles of MCS. The Total Number of Deterministic Analyses (TNDA) required to implement the ARBM is 94. Lower probabilities of failure of the frame for both LSFs in the presence of PR post-Northridge connections, indicates that they are stronger than FR connections. The study demonstrates the recommendation

Table 4 Uncertainty of RVs used for 3-story steel frame

RV	Mean (\bar{X})	Nominal (X_N)	\bar{X}/X_N	COV	Distribution
E (kN/m ²)	1.9995E+08	1.9995E+08	1.00	0.06	Lognormal
F_{yG} (kN/m ²)*	3.3509E+05	2.4821E+05	1.35	0.10	Lognormal
F_{yC} (kN/m ²)*	3.9645E+05	3.4474E+05	1.15	0.10	Lognormal
A (m ²)	***	**	1.00	0.05	Lognormal
I_x (m ²)	***	**	1.00	0.05	Lognormal
DL_1 (kN/m ²)	4.1727	3.9740	1.05	0.10	Normal
DL_2 (kN/m ²)	4.8263	4.5965	1.05	0.10	Normal
LL_1 (kN/m ²)	0.9576	2.3940	0.40	0.25	Type 1
LL_2 (kN/m ²)	0.9576	2.3940	0.40	0.25	Type 1
K (kN-m/rad)	****	**	1.00	0.15	Normal
K_p (kN-m/rad)	****	**	1.00	0.15	Normal
Mo (kN-m)	****	**	1.00	0.15	Normal
N_C	****	**	1.00	0.05	Normal
g_e	1.00	1.00	1.00	0.20	Type 1

*Yield stress of girder or column cross section reported in FEMA-355C [5].

**Nominal value (X_N) is calculated using mean value (\bar{X}) and \bar{X}/X_N .

***Mean values of A and I_x can be found in steel construction manual (AISC, 2011). They are considered RVs for every girder and column.

****Mean values of four Richard parameters are reported in Table 5.

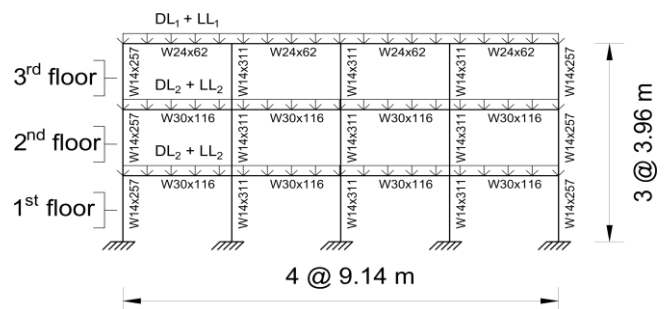


Fig. 10 Illustration of the 3-Story building

documented by the Structural Engineers Association of California (SEAOC) that post-Northridge steel connections improve the seismic performance of structures (FEMA-351, 2000; FEMA-352). In addition, for every case, the p_f obtained using the ARBM and MCS are very similar demonstrating that the ARBM is considerably accurate. In addition, results also indicate that when the ARBM is used, reliability information can be extracted using only 94 TNDA instead of 50,000 corresponding to MCS.

6.2 Application in performance-based seismic design

Table 5 Four Richard parameters for the 3-story building considering post-Northridge connections

Building Level*	Girder	Four Richard Parameters			N_c
		K (kN-m/rad)	K_p (kN-m/rad)	M_o (kN-m)	
Roof	W24X62	8.6433E+06	4.5194E+03	8.1519E+02	1.00
3-Story	3 W30X116	2.1354E+07	4.5194E+03	2.2134E+03	1.00
	2 W30X116	2.1354E+07	4.5194E+03	2.2134E+03	1.00

*See Fig. 10 for more details.

Once the accuracy of the ARBM has been properly validated, it is now important to document or showcase its implementation potential in PBSO. To achieve this objective, a 3-story steel building designed by experts in the

Los Angeles area is studied. It is illustrated in Fig. 10. The corresponding structural members are illustrated in the same Figure; as documented in FEMA-355C (2000).

Information related to RVs and uncertainty associated to the 3-story steel building, is presented in Table 4. The corresponding k value for the 3-story building is 25. Then, k_r is found to be 7. Since the SEAOC recommended to use post-Northridge PR connections (Fig. 9(b)), they are considered for the seismic risk evaluation of the 3-story steel frame. The four parameters of the Richard model corresponding to the 3-story building are summarized in Table 5. In order to study the beneficial effect of using post-Northridge connections, the steel structure is analyzed considering FR and PR (post-Northridge) connections.

To consider the large amount of uncertainty in both the amplitude and frequency contents of earthquakes, three suites of ground motions recommended by Somerville (1997) are used to excite the previously introduced 3-story

Table 6 Suite of ground motions corresponding to 2% probability of exceedance in 50 years and CP

EQ	Name	Mw	SF	PGA (g)	Time (sec)	Inter-Story Drift		Overall Lateral Drift	
						FR	PR	FR	PR
						β (TNDA)	β (TNDA)	β (TNDA)	β (TNDA)
1	1995 Kobe	6.9	1.15	1.282	25.0	8.393 (239)	8.761 (209)	7.720 (209)	8.005 (239)
2	1995 Kobe	6.9	1.15	0.920	25.0	9.512 (209)	9.790 (209)	9.388 (209)	10.972 (209)
3	1989 Loma Prieta	7.0	0.82	0.418	20.0	5.925 (209)	5.374 (239)	5.745 (209)	4.125 (209)
4	1989 Loma Prieta	7.0	0.82	0.473	20.0	8.571 (209)	8.524 (209)	8.380 (209)	8.180 (209)
5	1994 Northridge	6.7	1.29	0.868	14.0	5.836 (209)	5.896 (209)	6.415 (209)	6.523 (209)
6	1994 Northridge	6.7	1.29	0.943	14.0	7.681 (209)	8.169 (239)	9.563 (209)	8.486 (209)
7	1994 Northridge	6.7	1.61	0.926	15.0	8.709 (209)	9.021 (209)	11.204 (209)	11.634 (209)
8	1994 Northridge	6.7	1.61	1.329	15.0	5.520 (209)	5.475 (209)	3.880 (209)	3.922 (209)
9	1974 Tabas	7.4	1.08	0.808	25.0	4.962 (209)	5.480 (239)	5.826 (209)	6.638 (209)
10	1974 Tabas	7.4	1.08	0.991	25.0	5.814 (209)	5.972 (209)	6.282 (209)	6.399 (239)
11	Elysian Park (simulated)	7.1	1.43	1.295	18.0	4.742 (209)	5.010 (209)	5.346 (209)	5.537 (209)
12	Elysian Park (simulated)	7.1	1.43	1.186	18.0	7.060 (239)	7.721 (239)	8.622 (209)	9.530 (209)
13	Elysian Park (simulated)	7.1	0.97	0.782	18.0	9.209 (209)	8.598 (209)	9.584 (209)	10.463 (209)
14	Elysian Park (simulated)	7.1	0.97	0.680	18.0	7.805 (209)	8.643 (209)	8.467 (209)	9.451 (209)
15	Elysian Park (simulated)	7.1	1.10	0.991	18.0	5.478 (209)	5.818 (209)	6.741 (209)	6.732 (209)
16	Elysian Park (simulated)	7.1	1.10	1.100	18.0	8.748 (239)	8.778 (209)	8.362 (209)	6.282 (209)
17	Palos Verdes (simulated)	7.1	0.90	0.711	25.0	7.385 (209)	7.279 (209)	9.535 (209)	9.963 (209)
18	Palos Verdes (simulated)	7.1	0.90	0.776	25.0	8.782 (239)	9.842 (209)	9.373 (224)	11.034 (209)
19	Palos Verdes (simulated)	7.1	0.88	0.500	25.0	7.266 (209)	7.714 (209)	7.004 (209)	8.824 (209)
20	Palos Verdes (simulated)	7.1	0.88	0.625	25.0	6.611 (239)	6.093 (209)	5.878 (224)	4.753 (224)

Table 7 Suite of ground motions corresponding to 10% probability of exceedance in 50 years and LS

EQ	Name	Mw	SF	PGA (g)	Time (sec)	Inter-Story Drift		Overall Lateral Drift	
						FR	PR	FR	PR
						β (TNDA)	β (TNDA)	β (TNDA)	β (TNDA)
21	Imperial Valley, 1940	6.9	2.01	0.461	25.0	9.156 (224)	9.431 (209)	4.929 (209)	5.605 (209)
22	Imperial Valley, 1940	6.9	2.01	0.675	25.0	4.777 (209)	4.643 (209)	6.804 (209)	7.172 (209)
23	Imperial Valley, 1979	6.5	1.01	0.393	15.0	8.105 (209)	8.295 (209)	4.180 (224)	4.332 (209)
24	Imperial Valley, 1979	6.5	1.01	0.488	15.0	6.789 (209)	6.732 (209)	7.636 (209)	7.321 (209)
25	Imperial Valley, 1979	6.5	0.84	0.301	15.0	10.083 (224)	10.668 (209)	7.594 (209)	7.117 (209)
26	Imperial Valley, 1979	6.5	0.84	0.234	15.0	7.976 (224)	8.156 (209)	6.115 (209)	6.020 (209)
27	Landers, 1992	7.3	3.20	0.421	30.0	8.505 (224)	8.540 (209)	6.725 (224)	6.720 (209)
28	Landers, 1992	7.3	3.20	0.425	30.0	9.884 (224)	10.199 (209)	9.284 (209)	11.395 (209)
29	Landers, 1992	7.3	2.17	0.519	30.0	9.072 (209)	9.608 (209)	7.774 (224)	7.443 (209)
30	Landers, 1992	7.3	2.17	0.360	30.0	9.811 (209)	8.912 (209)	10.246 (209)	9.776 (209)
31	Loma Prieta, 1989	7.0	1.79	0.665	16.0	8.491 (209)	8.455 (224)	5.638 (209)	5.729 (209)
32	Loma Prieta, 1989	7.0	1.79	0.969	16.0	6.047 (209)	6.128 (224)	4.061 (209)	4.189 (224)
33	Northridge, 1994, Newhall	6.7	1.03	0.678	15.0	4.126 (209)	4.457 (209)	4.583 (209)	4.900 (209)
34	Northridge, 1994, Newhall	6.7	1.03	0.657	15.0	8.141 (209)	8.706 (224)	4.736 (209)	5.820 (209)
35	Northridge, 1994, Rinaldi	6.7	0.79	0.533	14.0	4.960 (224)	5.023 (209)	5.520 (209)	5.613 (209)
36	Northridge, 1994, Rinaldi	6.7	0.79	0.579	14.0	8.898 (209)	9.374 (209)	8.521 (209)	8.865 (209)
37	Northridge, 1994, Sylmar	6.7	0.99	0.569	15.0	9.661 (209)	10.774 (209)	3.720 (209)	4.771 (209)
38	Northridge, 1994, Sylmar	6.7	0.99	0.817	15.0	4.559 (209)	4.612 (209)	3.103 (209)	3.144 (209)
39	North Palm Springs, 1986	6.0	2.97	1.018	16.0	5.738 (224)	5.724 (209)	4.164 (224)	3.915 (209)
40	North Palm Springs, 1986	6.0	2.97	0.986	16.0	5.592 (209)	6.511 (209)	2.727 (209)	4.660 (209)

steel building. Tables 6-8 summarize the three suites of ground motions proposed by Somerville (1997) in terms of earthquake number (EQ), name, magnitude (Mw), scale factor (SF), peak ground acceleration (PGA), and excitation time (Time), respectively. More details about these suites of ground motions can be found in the literature (Somerville, 1997). Every suite consists of ten (each with two orthogonal components) ground motions representing return periods of 2475-year (2% probability of exceedance in 50 years, representing CP performance level), 475-year (10% probability of exceedance in 50 years, representing LS performance level), and 72-year (50% probability of exceedance in 50 years, representing IO performance level), respectively. Structural reliability results in terms of β and TNDA corresponding to CP (EQ-1 to EQ-20), LS (EQ-21 to EQ-40), and IO (EQ-41 to EQ-60) performance levels are summarized in Tables 6-8, respectively. Both LSFs overall lateral and inter-story drift are considered in the reliability

analysis. For the corresponding overall lateral drift, allowable values of 59.44, 29.72, and 8.32 cm are considered for CP, LS, and IO, respectively. Risk related to inter-story drift is calculated considering the 2nd floor, using permissible values equal to 19.81, 9.91, 2.77 cm corresponding to CP, LS, and IO, respectively. Allowable deflection limits are recommended in PBSD guidelines (FEMA-350, 2000), depending on the total and inter-story heights of the structure under consideration.

Several observations can be made related to results presented in Tables 6-8. The β values are very different when the structure is excited by every earthquake time history. This is expected since the frequency contents of each record are different. Thus, designing a structure for one earthquake time history is inadequate. This observation justifies the use of multiple time histories to design a structure; as suggested in more recent design guidelines (ASCE/SEI 7-16, 2017). In addition, β values for FR

Table 8 Suite of ground motions corresponding to 50% probability of exceedance in 50 years and IO

EQ	Name	Mw	SF	PGA (g)	Time (sec)	Inter-Story Drift		Overall Lateral Drift	
						FR	PR	FR	PR
						β (TNDA)	β (TNDA)	β (TNDA)	β (TNDA)
41	Coyote Lake, 1979	5.7	2.28	0.589	12.0	1.548 (209)	1.644 (209)	2.145 (224)	2.230 (209)
42	Coyote Lake, 1979	5.7	2.28	0.333	12.0	5.873 (209)	5.851 (224)	6.510 (209)	6.483 (224)
43	Imperial Valley, 1979	6.5	0.40	0.143	15.0	9.621 (224)	9.964 (224)	8.993 (209)	9.184 (209)
44	Imperial Valley, 1979	6.5	0.40	0.112	15.0	9.142 (209)	9.762 (224)	10.014 (224)	10.537 (209)
45	Kern, 1952	7.7	2.92	0.144	30.0	7.423 (209)	7.555 (224)	8.020 (209)	8.304 (209)
46	Kern, 1952	7.7	2.92	0.159	30.0	7.863 (224)	8.025 (224)	8.685 (209)	8.895 (224)
47	Landers, 1992	7.3	2.63	0.337	25.0	3.704 (209)	3.885 (209)	4.217 (209)	4.393 (209)
48	Landers, 1992	7.3	2.63	0.307	25.0	5.559 (224)	6.000 (209)	6.404 (209)	6.981 (209)
49	Morgan Hill, 1984	6.2	2.35	0.318	20.0	4.584 (209)	4.686 (209)	6.905 (209)	6.207 (224)
50	Morgan Hill, 1984	6.2	2.35	0.546	20.0	4.529 (209)	4.504 (224)	5.105 (224)	5.088 (224)
51	Parkfield, 1966, Cholame	6.1	1.81	0.780	15.0	1.568 (224)	1.584 (209)	2.162 (209)	2.174 (224)
52	Parkfield, 1966, Cholame	6.1	1.81	0.631	15.0	1.561 (209)	1.652 (209)	2.140 (209)	2.219 (224)
53	Parkfield, 1966, Cholame	6.1	2.92	0.693	15.0	4.266 (209)	4.290 (224)	4.853 (209)	4.922 (209)
54	Parkfield, 1966, Cholame	6.1	2.92	0.790	15.0	2.766 (224)	2.843 (209)	3.297 (224)	3.368 (209)
55	North Palm Springs, 1986	6.0	2.75	0.517	20.0	5.086 (209)	5.331 (209)	5.681 (209)	5.994 (209)
56	North Palm Springs, 1986	6.0	2.75	0.379	20.0	5.611 (209)	5.918 (224)	7.650 (209)	7.864 (224)
57	San Fernando, 1971	6.5	1.30	0.253	20.0	6.362 (224)	6.947 (209)	7.076 (224)	7.845 (224)
58	San Fernando, 1971	6.5	1.30	0.231	20.0	7.598 (209)	7.276 (224)	7.989 (209)	7.930 (209)
59	Whittier, 1987	6.0	3.62	0.768	15.0	2.347 (224)	2.433 (224)	2.284 (209)	2.603 (224)
60	Whittier, 1987	6.0	3.62	0.478	15.0	1.892 (224)	2.104 (209)	2.404 (224)	2.601 (209)

connections are very similar to those of PR using post-Northridge connections. Furthermore, it can be observed in Tables 6-8 that only hundreds of TNDA are required for extracting the corresponding reliability information. In addition, it can be justified that the permissible displacement values suggested in FEMA-350 (2000) are reasonable. The β values fall within a tolerable range, satisfying the intent of the code (ASCE/SEI 7-16 2017). For the ease of discussions, the mean, $\beta\mu$, values and corresponding p_f are given in Table 9. Generally, $\beta\mu$ values are observed to be the highest for the CP and LS performance levels and lowest for the IO performance level, confirming the intent of the PBSG guidelines (FEMA-350, 2000). It is also interesting to note the distinct separations of performance levels of CP, LS, and IO. This indicates that the SFs to match target spectral values at certain frequencies are rational (Somerville 1997). Also, results summarized in Table 9 demonstrate that the performance of

Table 9 Mean structural reliability ($\beta\mu$) and p_f corresponding to 3-story building

Performance Level	Overall Lateral Drift		Inter-Story Drift	
	FR	PR	FR	PR
	$\beta\mu$ (p_f)			
CP (2475-Year Return Period)	7.666 (8.8818E-15)	7.873 (1.7764E-15)	7.200 (3.0109E-13)	7.398 (6.9167E-14)
LS (475-Year Return Period)	5.903 (1.7848E-09)	6.225 (2.4078E-10)	7.518 (2.7756E-14)	7.747 (4.6629E-15)
IO (72-Year Return Period)	5.627 (9.1685E-09)	5.791 (3.4984E-09)	4.945 (3.8072E-07)	5.113 (1.5854E-07)

the structure when connections are considered to be FR and post-Northridge PR type are very similar. In fact, the study indicates that post-Northridge connections improve the structural behavior, providing better reliability than FR connections.

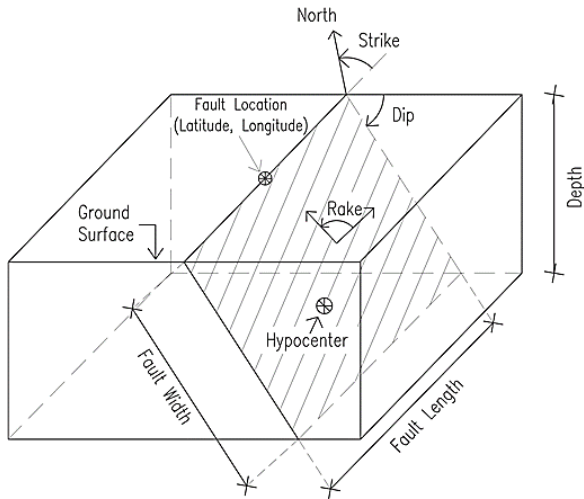


Fig. 11 Illustration of rupture

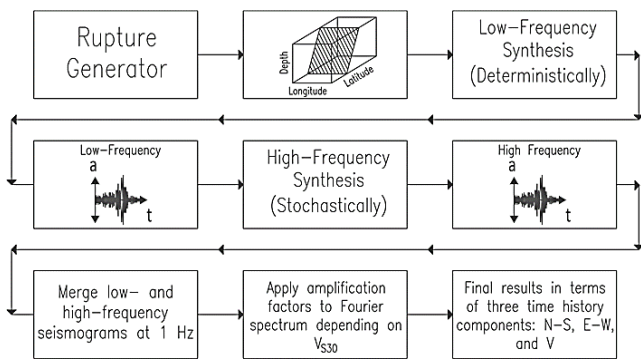
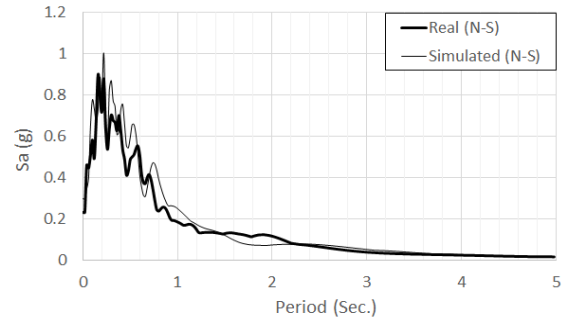


Fig. 12 Flowchart of the BBP process

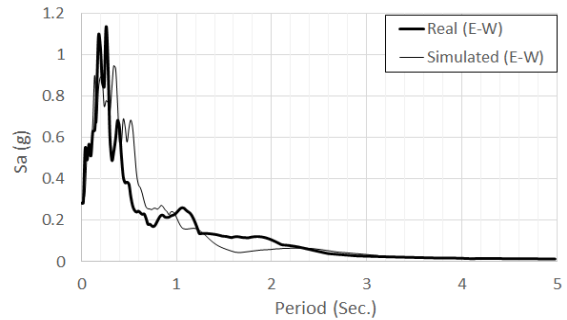
6.3 Safety evaluation using real and simulated ground motions

The ARBM has been properly validated using MCS, and its implementation potential was showcased for problems related to PBSO. In this part, the BBP developed by the SCEC is used for the proper simulation of ground motions (SCEC 2016). The BBP is an open source software developed by the SCEC for hybrid broadband simulation of ground motions (SCEC 2016). Several researchers have developed modules of the BBP for nonlinear site effects, low and high frequency seismogram synthesis, and rupture generation (Zeng *et al.* 1994, Motazedian and Atkinson 2005, Schmedes *et al.* 2010, Mai *et al.* 2010, Graves and Pitarka 2010). In order to simulate ground motions using the BBP, a single-plane fault surface should be generated as illustrated in Fig. 11.

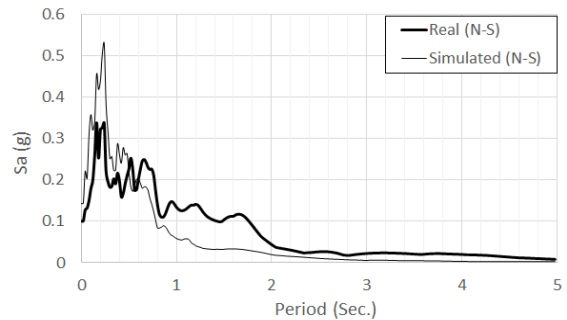
A simple description of the rupture is defined by the user in terms of hypocenter location, magnitude, rupture dimensions, dip, strike, and rake (see Fig. 11). This information is used by the BBP rupture generator module and a detailed time history of slip on the rupture surface is created. A list of stations where ground motion time histories will be simulated is also provided by the user in terms of latitude, longitude, and V_{S30} (shear wave velocity of the top 30 m of the subsurface profile) of the specific site. Both low- and high-frequency synthesis modules compute deterministically and stochastically frequency



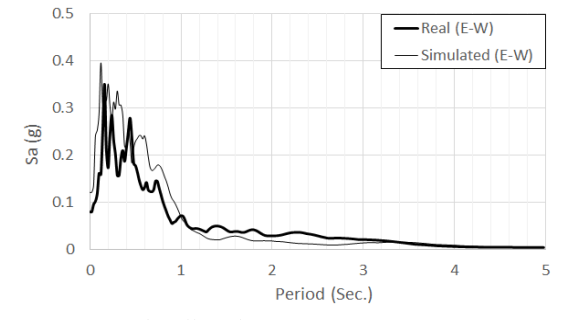
(a) Santa Susana N-S



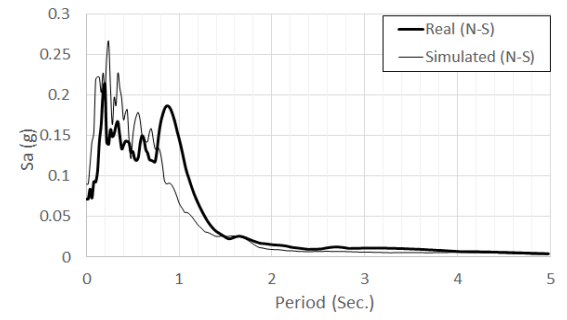
(b) Santa Susana E-W



(c) Alhambra - Fremont N-S

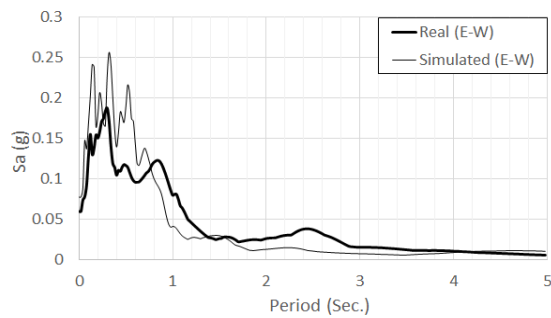


(d) Alhambra - Fremont E-W

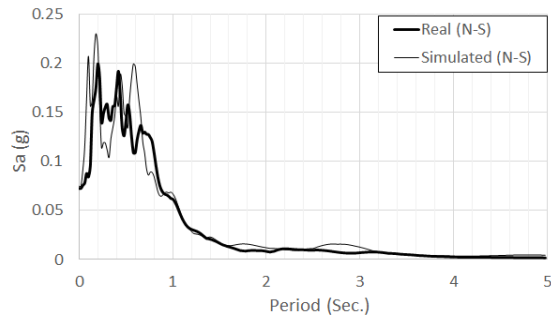


(e) Littlerock - Brainard N-S

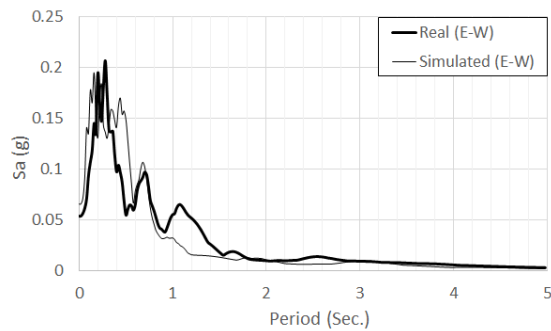
Fig. 13 Real and simulated response spectra of the 1994 Northridge earthquake



(f) Littlerock - Brainard E-W



(g) Rancho Palos Verdes N-S



(h) Rancho Palos Verdes E-W

Fig. 13 Continued

seismograms, respectively. Such seismograms are then merged together at a frequency of approximately 1 Hz. Furthermore, an empirical site amplification is applied to its Fourier spectrum depending on the corresponding target value of V_{S30} . At the end, results are reported for every station in terms of three acceleration time histories: North-South (N-S), East-West (E-W), and Vertical (V). The BBP sequential process is illustrated in Fig. 12.

To validate the BBP, four locations in southern California are selected where real time histories of the 1994 Northridge earthquake are available. They are: (1) Santa Susana, (2) Alhambra – Fremont, (3) Littlerock – Brainard, and (4) Rancho Palos Verdes. Using the BBP v16.5.0 (SCEC 2016) and Graves and Pitarka method (Graves and Pitarka 2010), simulations corresponding to the 1994 Northridge earthquake are performed for the above four stations. The rupture was generated using a magnitude of 6.7, fault length and width equal to 20 and 27 km, respectively. Strike, rake, and dip were considered as 122° , 105° , and 40° , respectively. Fig. 13 illustrates the corresponding response spectra for real and simulated

Table 10 Structural reliability for real and simulated ground motions evaluating 2-story steel frame

Station	Overall Lateral Drift		Inter-Story Drift	
	Real	Simulated	Real	Simulated
	β	β	β	β
Santa Susana N-S	3.6137	3.9556	3.0545	3.0810
Santa Susana E-W	3.8067	3.6250	3.4565	3.3591
Alhambra - Fremont N-S	4.2430	4.3176	4.1201	4.3594
Alhambra - Fremont E-W	5.2484	5.4095	5.4044	5.3108
Littlerock -Brainard N-S	3.8286	3.2042	3.8287	3.2146
Littlerock -Brainard E-W	4.2997	4.1296	3.8521	3.1554
Rancho Palos Verdes N-S	4.8866	4.6424	3.8442	3.3492
Rancho Palos Verdes E-W	3.5370	3.3994	3.8271	3.8622
β_μ	4.1830	4.0854	3.9235	3.7115
(p_f)	(1.4384E-05)	(2.2000E-05)	(4.3636E-05)	(1.0302E-04)

versions of the 1994 Northridge earthquake. Response spectra are plotted considering the N-S and E-W components of every station under study. It can be observed in Fig. 13 that response spectra for simulated and real ground motions are very similar. To evaluate the accuracy in terms of risk, the 2-Story steel frame shown earlier in Fig. 9(a) is excited using real and simulated versions of the 1994 Northridge earthquake as illustrated in Fig. 13.

Risk is obtained using the proposed ARBM. The corresponding RVs were summarized earlier in Table 2. Since one of the objectives of this paper is to demonstrate the applicability of the ARBM using simulated and real ground motions, for this numerical example, only FR connections are considered for the reliability analysis of the 2-story frame. Table 10 summarizes the results of the structural reliability using simulated and real ground motions, respectively. It can be observed that β and p_f are very similar for simulated and real versions of ground motions. In terms of mean reliability index (β_μ), it can be observed that the performance of the building is more critical for inter-story drift conditions. Based on the results presented in this section, the accuracy of the BBP version v16.5.0 (SCEC 2016) is validated in terms of response spectra and associated reliability.

7. Conclusions

The alternative reliability-based methodology is found to be very efficient and accurate for risk calculation using real and simulated ground motions. In such methodology, structures are represented by finite elements and seismic loading is applied in time domain. Major sources of nonlinearity and uncertainty are incorporated in the formulation. Based on the results and technical contents of this paper, several comments and conclusions can be identified. They are listed next.

- The applicability of the alternative reliability-based

methodology is demonstrated. The capabilities of the technique are expected to be acceptable to all concerned parties and can be used for routine applications.

- Using the alternative reliability-based methodology, the structural risk can be obtained using hundreds instead of several thousands of deterministic analyses. This methodology may represent an alternative to MCS and the classical random vibration methods.
- A type of post-Northridge PR connection considered in this study appears to have many desirable characteristics. It may contribute to make steel structures more seismic load-tolerant.
- The study confirms that designing structures using multiple time histories, as suggested in recent design guidelines, is a step in the right direction. Multiple deterministic analyses considering major sources of nonlinearity and uncertainty are required to make a structure more damage-tolerant.
- The BBP version v16.5.0 is demonstrated to be a viable option for the proper simulation of ground motions. Its accuracy in terms of structural risk is demonstrated.

Acknowledgments

The first author would like to thank to Prof. A. Haldar, Prof. A. Reyes-Salazar, Prof. J. Ignacio Velazquez-Dimas, Prof. A. Omar Vazquez-Hernandez, and Prof. G. Esteban Vazquez-Becerra for all the support provided to the first author in obtaining his MS and PhD. In addition, many thanks are given to the unknown reviewers, time and effort revising this paper are tremendously appreciated. This work was financially supported by several agencies of the government of Mexico: *Consejo Nacional de Ciencia y Tecnología* (CONACYT), *Universidad Autónoma de Sinaloa* (UAS), *Dirección General de Relaciones Internacionales de la Secretaría de Educación Pública* (DGRI-SEP). The study is also partially supported by the National Science Foundation under Grant No. CMMI-1403844. Any opinions, findings, or recommendations expressed in this paper are those of the authors and do not necessarily reflect the views of the sponsors.

References

- AISC (2011), *Steel Construction Manual*, American Institute of Steel Construction (AISC).
- AISC 341-10 (2010), *Seismic Provisions for Structural Steel Buildings*, American Institute of Steel Construction (AISC).
- Ang, A.H.S. and Cornell, C.A. (1974), "Reliability bases of structural safety and design", *J. Struct. Div.*, **100**(9), 1755-1769.
- ASCE/SEI 41-13 (2014), *Seismic Evaluation and Retrofit of Existing Buildings*, American Society of Civil Engineers (ASCE), Reston, VA, USA.
- ASCE/SEI 7-16 (2017), *Minimum Design Loads for Buildings and Other Structures*, American Society of Civil Engineers (ASCE), Reston, VA, USA.
- Azizoltani, H. and Haldar, A. (2017a), "A surrogate concept of multiple deterministic analyses of non-linear structures excited by dynamic loadings", *Proceedings of the 12th International Conference on Structural Safety & Reliability*, Vienna, Austria.
- Azizoltani, H. and Haldar, A. (2017b), "Intelligent computational schemes for designing more seismic damage-tolerant structures", *J. Earthq. Eng.*, 1-28.
- Azizoltani, H., Gaxiola-Camacho, J.R., and Haldar, A. (2018), "Site-specific seismic design of damage tolerant structural systems using a novel concept", *B. Earthq. Eng.*, 1-25.
- Box, G.E., Hunter, W.G. and Hunter, J.S. (1978), *Statistics for Experimenters: An Introduction to Design, Data Analysis, and Model Building*, Wiley, New York, NY, USA.
- Burks, L.S., Zimmerman, R.B. and Baker, J.W. (2015), "Evaluation of hybrid broadband ground motion simulations for response history analysis and design", *Earthq. Spectra*, **31**(3), 1691-1710.
- Cacciola, P. and Deodatis, G. (2011), "A method for generating fully non-stationary and spectrum-compatible ground motion vector processes", *Soil Dyn. Earthq. Eng.*, **31**(3), 351-360.
- Cacciola, P. and Zentner, I. (2012), "Generation of response-spectrum-compatible artificial earthquake accelerograms with random joint time-frequency distributions", *Probab. Eng. Mech.*, **28**, 52-58.
- Chen, W.F. and Kishi, N. (1989), "Semirigid steel beam-to-column connections: Data base and modeling", *J. Struct. Eng.*, **115**(1), 105-119.
- Colson, A. (1991), "Theoretical modeling of semirigid connections behavior", *J. Constr. Steel Res.*, **19**(3), 213-224.
- Ellingwood, B. (1980), *Development of a Probability Based Load Criterion for American National Standard A58: Building Code Requirements for Minimum Design Loads in Buildings and Other Structures*, US Department of Commerce, National Bureau of Standards, Cambridge, MA, USA.
- Elsati, M.K. and Richard, P. (1996), "Derived moment rotation curves for partially restrained connections", *Struct. Eng. Rev.*, **8**(2-3), 151-158.
- Faravelli, L. (1989), "Response-surface approach for reliability analysis", *J. Eng. Mech.*, **115**(12), 2763-2781.
- FEMA-350 (2000), *Recommended Seismic Design Criteria for New Steel Moment-Frame Buildings*, Federal Emergency Management Agency (FEMA).
- FEMA-351 (2000), *Recommended Seismic Evaluation and Upgrade Criteria for Existing Welded Steel Moment-Frame Buildings*, Federal Emergency Management Agency (FEMA).
- FEMA-352 (2000), *Recommended Post-Earthquake Evaluation and Repair Criteria for Welded Steel Moment-Frame Buildings*, Federal Emergency Management Agency (FEMA).
- FEMA-353 (2000), *Recommended Specifications and Quality Assurance Guidelines for Steel Moment-Frame Construction for Seismic Applications*, Federal Emergency Management Agency (FEMA).
- FEMA-355C (2000), *State of the Art Report on Systems Performance of Steel Moment Frames Subject to Earthquake Ground Shaking*, Federal Emergency Management Agency (FEMA).
- FEMA-355F (2000), *State of the Art Report on Performance Prediction and Evaluation of Steel Moment-Frame Buildings*, Federal Emergency Management Agency (FEMA).
- FEMA P-58 (2012), *Seismic Performance Assessment of Buildings*, Federal Emergency Management Agency (FEMA).
- FEMA P-751 (2012), *NEHRP Recommended Seismic Provisions: Design Examples*, Federal Emergency Management Agency (FEMA).
- Gaxiola-Camacho, J.R., Azizoltani, H., Villegas-Mercado, F.J. and Haldar, A. (2017), "A novel reliability technique for implementation of Performance-Based Seismic Design of structures", *Eng. Struct.*, **142**, 137-147.
- Graves, R.W. and Pitarka, A. (2010), "Broadband ground-motion simulation using a hybrid approach", *Bull. Seismol. Soc. Am.*,

- 100(5A), 2095-2123.
- Haldar, A. and Mahadevan, S. (2000a), *Probability, Reliability, and Statistical Methods in Engineering Design*, Wiley, New York, NY, USA.
- Haldar, A. and Mahadevan, S. (2000b), *Reliability Assessment Using Stochastic Finite Element Analysis*, Wiley, New York, NY, USA.
- Hinton, E. and Owen, D.R.J. (1986), *Finite Elements in Plasticity: Theory and Practice*, Pineridge Press, Swansea, UK.
- Khuri, A.I. and Cornell, J.A. (1996), *Response Surfaces: Designs and Analyses*, Marcel Dekker, New York, NY, USA.
- LATBSDC (2011), An Alternative Procedure for Seismic Analysis and Design of Tall Buildings Located In the Los Angeles Region, Los Angeles Tall Buildings Structural Design Council (LATBSDC).
- Mai, P.M., Imperatori, W. and Olsen, K.B. (2010), "Hybrid broadband ground-motion simulations: Combining long-period deterministic synthetics with high-frequency multiple S-to-S backscattering", *Bull. Seismol. Soc. Am.*, **100**(5A), 2124-2142.
- Mehrabian, A., Ali, T. and Haldar, A. (2009), "Nonlinear analysis of a steel frame", *Nonlin. Anal. Theor. Meth. Appl.*, **71**(12), e616-e623.
- Mehrabian, A., Haldar, A. and Reyes-Salazar, A. (2005), "Seismic response analysis of steel frames with post-North ridge connection", *Steel Compos. Struct.*, **5**(4), 271-287.
- Motazedian, D. and Atkinson, G.M. (2005), "Stochastic finite-fault modeling based on a dynamic corner frequency", *Bull. Seismol. Soc. Am.*, **95**(3), 995-1010.
- Nowak, A.S. and Collins, K.R. (2012), *Reliability of Structures*, CRC Press, Boca Raton, FL, USA.
- Reyes-Salazar, A. and Haldar, A. (1999), "Nonlinear seismic response of steel structures with semi-rigid and composite connections", *J. Constr. Steel Res.*, **51**(1), 37-59.
- Reyes-Salazar, A., Ruiz, S.E., Bojorquez, E., Bojorquez, J. and Llanes-Tizoc, M.D. (2016a), "Seismic response of complex 3D steel buildings with welded and post-tensioned connections", *Earthq. Struct.*, **11**(2), 217-243.
- Reyes-Salazar, A., Soto-Lopez, M.E., Gaxiola-Camacho, J.R., Bojorquez, E. and Lopez-Barraza, A. (2014), "Seismic response estimation of steel buildings with deep columns and PMRF", *Steel Compos. Struct.*, **17**(4), 471-495.
- Reyes-Salazar, A., Valenzuela-Beltran, F., De Leon-Escobedo, D., Bojorquez-Mora, E. and Barraza, A.L. (2016b), "Combination rules and critical seismic response of steel buildings modeled as complex MDOF systems", *Earthq. Struct.*, **10**(1), 211-238.
- SCEC (2016), Broadband Platform; Southern California Earthquake Center (SCEC), USA.
- Schmedes, J., Archuleta, R.J. and Lavallee, D. (2010), "Correlation of earthquake source parameters inferred from dynamic rupture simulations", *J. Geophys. Res. Solid Earth*, **115**(B3), <https://doi.org/10.1029/2009JB006689>.
- Shields, M.D. (2014), "Simulation of spatially correlated nonstationary response spectrum-compatible ground motion time histories", *J. Eng. Mech.*, **141**(6), 04014161.
- Shinozuka, M. and Deodatis, G. (1988), "Stochastic process models for earthquake ground motion", *Probab. Eng. Mech.*, **3**(3), 114-123.
- Somerville, P.G. (1997) "Development of ground motion time histories for phase 2 of the FEMA/SAC steel project", SAC Joint Venture, Federal Emergency Management Agency (FEMA).
- Suarez, L.E. and Montejo, L.A. (2005), "Generation of artificial earthquakes via the wavelet transform", *Int. J. Solid. Struct.*, **42**(21), 5905-5919.
- TBI (2010), Guidelines for Performance-Based Seismic Design of Tall Buildings, Pacific Earthquake Engineering Research Center, Tall Buildings Initiative (TBI).
- Yamamoto, Y. and Baker, J.W. (2013), "Stochastic model for earthquake ground motion using wavelet packets", *Bull. Seismol. Soc. Am.*, **103**(6), 3044-3056.
- Zeng, Y., Anderson, J.G. and Yu, G. (1994), "A composite source model for computing realistic synthetic strong ground motions", *Geophys. Res. Lett.*, **21**(8), 725-728.

AT

List of acronyms

PBSD	Performance-Based Seismic Design
FE	Finite Element
FEM	Finite Element Method
PR	Partially Restrained
FR	Fully Restrained
FORM	First Order Reliability Method
MVFOSM	Mean Value First-Order Second-Moment
MCS	Monte Carlo Simulation
LSF	Limit State Function
PDF	Probability Density Function
CDF	Cumulative Density Function
RV	Random Variable
BBP	Broadband Platform
SCEC	Southern California Earthquake Center
MPFP	Most Probable Failure Point
SD	Saturated Design
CCD	Central Composite Design
DL	Dead Load
LL	Live Load
ARBM	Alternative Reliability-Based Methodology
IO	Immediate Occupancy
LS	Life Safety
CP	Collapse Prevention
TNDA	Total Number of Deterministic Analyses